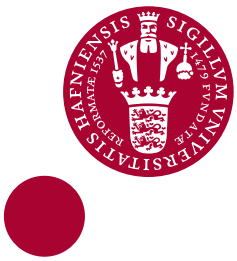

Dynamics of intracellular mannan and cell wall folding in the drought responses of succulent Aloe species

Isager Ahl, Louise; Mravec, Jozef; Jørgensen, Bodil; Rudall, Paula J.; Rønsted, Nina; Grace, Olwen M

Published in:
Plant, Cell and Environment

DOI:
10.1111/pce.13560

Publication date:
2019

Document version
Publisher's PDF, also known as Version of record

Received: 5 February 2019 | Revised: 29 March 2019 | Accepted: 1 April 2019

DOI: 10.1111/pce.13560

ORIGINAL ARTICLE

WILEY Plant, Cell & Environment

Dynamics of intracellular mannan and cell wall folding in the drought responses of succulent *Aloe* species

Louise Isager Ahl[1] | Jozef Mravec[2] | Bodil Jørgensen[2] | Paula J. Rudall[3] | Nina Rønsted[1] | Olwen M. Grace[3]

[1] Natural History Museum of Denmark, Faculty of Science, University of Copenhagen, Copenhagen K DK-1353, Denmark

[2] Department of Plant and Environmental Sciences, Faculty of Science, University of Copenhagen, Frederiksberg C DK-1871, Denmark

[3] Department of Comparative Plant and Fungal Biology, Royal Botanic Gardens, Kew, Richmond TW9 3AE, UK

Correspondence
L. I. Ahl, Natural History Museum of Denmark, Faculty of Science, University of Copenhagen, Øster Farimagsgade 5, Copenhagen K DK-1353, Denmark.
Email: louise.ahl@snm.ku.dk

Funding information
Carlsberg Foundation, Grant/Award Number: CF17-0181; Villum Foundation, Grant/Award Numbers: 17489 and 9283

Abstract

Plants have evolved a multitude of adaptations to survive extreme conditions. Succulent plants have the capacity to tolerate periodically dry environments, due to their ability to retain water in a specialized tissue, termed hydrenchyma. Cell wall polysaccharides are important components of water storage in hydrenchyma cells. However, the role of the cell wall and its polysaccharide composition in relation to drought resistance of succulent plants are unknown. We investigate the drought response of leaf-succulent *Aloe* (Asphodelaceae) species using a combination of histological microscopy, quantification of water content, and comprehensive microarray polymer profiling. We observed a previously unreported mode of polysaccharide and cell wall structural dynamics triggered by water shortage. Microscopical analysis of the hydrenchyma cell walls revealed highly regular folding patterns indicative of predetermined cell wall mechanics in the remobilization of stored water and the possible role of homogalacturonan in this process. The in situ distribution of mannans in distinct intracellular compartments during drought, for storage, and apparent upregulation of pectins, imparting flexibility to the cell wall, facilitate elaborate cell wall folding during drought stress. We conclude that cell wall polysaccharide composition plays an important role in water storage and drought response in *Aloe*.

KEYWORDS

adaptation, *Aloe*, CoMPP, drought, hydrenchyma, leaf anatomy, morphology, plant cell walls, polysaccharides, succulence

1 | INTRODUCTION

The remarkable diversification success of land plants has been attributed to the evolution of adaptations to cope with potential abiotic stressors such as drought, temperature, and light (Raven, Evert, & Eichhorn, 2005). In desert environments, plants must be able to cope with all three factors (Moore, Vicré-Gibouin, Farrant, & Driouich, 2008). The ability to store and use water in a regulated manner is a remarkable and crucial adaptation in the ecological success of succulent plants (Grace, 2019), which are estimated to include *ca*. 12,000 species in diverse lineages of the angiosperm tree of life (Moore et al., 2008; Nyffeler & Eggli, 2009).

Succulent plants typically possess thick and fleshy leaves and/or stems as an adaptation to periodically dry environments (Landrum,

Louise Isager Ahl and Jozef Mravec should be considered joint first authors.

2002; Males, 2017; Ogburn & Edwards, 2010). The first morphological studies of *Aloe* and other succulents were published in the late 18th century (Haberlandt, 1914; Pfitzer, 1877). In leaf succulents such as *Aloe*, the inner leaf mesophyll cells are typically large and thin walled with large central vacuoles, and lack chloroplasts. These cells comprise the specialized hydrenchyma tissue (Beaumont, Cutler, Reynolds, & Vaughan, 1985; Schmidt & Kaiser, 1987). The hydrenchyma is surrounded by photosynthetic tissue (chlorenchyma), which in turn is contained within the epidermis; a thick cuticle overlying the epidermis provides further protection against dehydration (Kluge & Ting, 1978; Wiebe & Al-Saadi, 1976). The relatively large size of the cells and vacuoles of the hydrenchyma tissue allows succulent plants to hold larger amounts of water than less specialized mesophyll cells. When water is scarce, stored water is reallocated from the hydrenchyma to the photosynthetic chlorenchyma. The movement of water is aided by contraction of the radial walls, which pushes it outwards into the surrounding chlorenchyma (Haberlandt, 1914; Lambers, Chapin, & Pons, 1998; Ripley, Abraham, Klak, & Cramer, 2013; Wiebe & Al-Saadi, 1976). Increased elasticity of the hydrenchyma cell walls enables these cells to expand when water is available and to contract during drought (Schmidt & Kaiser, 1987; von Willert, Eller, Werger, & Brinckmann, 1990; Becker, 2007). However, the underlying mechanism enabling cell wall contraction and expansion has remained largely unknown.

Polysaccharides are fundamental building blocks of plant cell walls, defining the strength, function, and properties of different plant tissues. The major polysaccharides constituting the cell walls are cellulose, hemicelluloses, and pectins (Albersheim, Darvill, Roberts, Sederoff, & Staehelin, 2011; Cosgrove, 2005, 2016). Cellulose microfibrils are long homogenous strands of β-1,4-linked glycosyl residues, tied together by hemicelluloses forming the cell wall scaffold; the entire complex is embedded in a pectin-rich matrix (Albersheim et al., 2011). Polysaccharides are also present between cells with pectins being the primary polysaccharide constituting the middle lamella, which itself is part of the apoplast, a local transport route of both water and solutes (Albersheim et al., 2011). Apoplastic polysaccharides could play an important role in how a plant responds to drought. They are also likely to be involved in the mechanistic link between crassulacean acid metabolism (CAM) and the water-regulatory system of a plant during a period of drought (von Willert et al., 1990; Pimienta-Barrios, González, Castillo-Aranda, & Nobel, 2002; Ogburn & Edwards, 2010, 2012). However, despite this potentially essential role in water storage, the composition and potential role of polysaccharides in hydrenchyma cells have not yet been systematically investigated in succulent plants.

Members of the leaf-succulent genus *Aloe* (Asphodelaceae) show considerable diversity in leaf succulence, ranging from barely succulent, in the so-called grass aloes, to highly succulent species such as the medicinal *Aloe ferox* Mill. and *Aloe vera* L. The succulent leaf tissue of *A. vera* is used worldwide, whereas other species are used locally (Grace, 2011). In a previous study by Ahl et al., two types of hemicelluloses were detected in this tissue of four different species of aloes—xyloglucans and mannans (Ahl et al., 2018, 2019). However, the pharmacological activity of *A. vera* is attributed only to acetylated mannan. Mannan is a linear polymer composed of D-mannose molecules linked together by β-(1,4) linkages, usually with molecular weight lower than 30 kDa (Reynolds & Dweck, 1999; Talmadge et al., 2004). Heteromannans are mannan derivatives built on variations of the β-mannan backbone, which is sometimes interrupted by D-glucose to form glucomannan and/or branched with α-(1,6)-linked D-galactose to form galactomannan (Chauhan, Puri, Sharma, & Gupta, 2012; Pauly et al., 2013).

Mannans are generally considered to function as structural cell wall polysaccharides providing increased hardness to plant tissues although in seeds they often function as storage polysaccharides (Buckeridge, 2010; Stancato, Buckeridge, & Mazzafera, 2001). In epiphytic orchids, glucomannans in the pseudobulb are involved in moderating the effects of water stress (Stancato et al., 2001). Mannan is also likely among the apoplastic polysaccharides that aid in the retention of water in the leaves of *Aloe* species during periods of drought (Kluge & Ting, 1978; Nyffeler & Eggli, 2009; Ogburn & Edwards, 2012; Wiebe & Al-Saadi, 1976).

Pectic polysaccharides are the primary components of the middle lamella; they form the gels that embed the cellulose and hemicellulose network (Cosgrove, 2016; Paulsen & Barsett, 2005; Willats, Knox, & Mikkelsen, 2006). Pectins can be structurally alternated into forming either very liquid or solid gels by modulations in the amount and distribution of methyl groups, the structure, length, and nature of the rhamnogalacturonan-I (RG-I) and rhamnogalacturonan-II side chains, and the extent and nature of the substitutions on the backbone (Sørensen, Pedersen, & Willats, 2009; Willats et al., 2006; Willats, Mccartney, Mackie, & Knox, 2001). Both mannans and pectins are therefore of particular interest in relation to cell wall flexibility in hydrenchyma cells of *Aloe* species.

To investigate the structure and mechanisms allowing succulent plants to thrive in desert environments, we utilized a novel combination of histological microscopy, water content measurement, and comprehensive microarray polymer profiling (CoMPP) to evaluate the effects of a 6-week artificial drought on cell wall polysaccharide composition in the succulent tissue of two species of *Aloe*: *Aloe helenae* Danguy and *A. vera* L.

2 | MATERIALS AND METHODS

2.1 | Growth conditions and sampling

Plant material of *A. helenae* Denguy (a tree Aloe, voucher number Ahl 96 deposited at C) and *A. vera* L. (a stemless Aloe, voucher number Ahl 94 deposited at C) was obtained from the living collections at the Botanic Garden of the Natural History Museum of Denmark, University of Copenhagen, Denmark. *A. helenae* was selected for its known visible reactions to drought stress (colour change and thinning of leaves), whereas *A. vera* was chosen for its adaptability to different growing conditions. An additional four species were included in the initial CoMPP screening (Figure S1).

Mature (>20 years old) plants of the two species were grown under glass in conditions mimicking the daylight changes and water availability of their natural habitat. Accordingly, irrigation is changed depending on the seasons and natural light of the Northern hemisphere, with more watering (2–3 times per week) in the summer (June–August) and less in the spring, autumn, and winter (0–2 times per week). Plants are regularly given Nitrogen Phosphor Potassium (NPK) fertilizer, and artificial light is supplied during the autumn and winter to resemble the light availability of the southern hemisphere, where most *Aloe* species originate. Finally, temperature is kept at a minimum of 13–17°C. Three plants were sampled for each species before and after exposure to drought (no watering), on August 01, 2017, and September 11, 2017, respectively. At the same time, three control plants watered according to the normal watering regime were sampled for each species. The drought experiment was repeated on the same plants between May 08, 2018, and June 19, 2018.

2.2 | Relative and SWC

Leaf cores were taken from the drought stressed and control species of *A. vera* and *A. helenae* in the greenhouse. Samples were taken between 12:00 p.m. and 1:00 p.m. in accordance with the original recommendations of Smart and Bingham (1974), as a standardized approach (Smart & Bingham, 1974). Two leaf core samples from each species were placed in preweighed tubes. Samples were weighed, and 1 ml of distilled water (dH_2O) was added to each tube, covering the samples completely. All samples were refrigerated at 5°C for 3–4 hr to all full rehydration. Excess water was removed before samples (and tubes) were weighed to obtain full turgid weight (TW). Tubes and samples were then incubated in an oven at 80°C for 62 hr with the lids off before they were weighed to obtain the dry weight (DW). All measurements were made in milligrams (mg) with two decimal places. For each species and treatment, calculations were made using the following formulas:

Calculation of relative water content (RWC) in %:

$$\text{RWC}\ (\%) = [(\text{W} - \text{DW}) \div (\text{TW} - \text{DW})] \times 100,$$

Calculation of saturated water content (SWC) in %:

$$\text{SWC}\ (\%) = [(\text{TW} - \text{DW}) \div (\text{DW})] \times 100,$$

where W is the fresh weight (mg), TW is the turgid weight (mg), and DW is the dry weight (mg).

2.3 | Microscopy

Thick transverse sections (0.5 cm^2) were carefully excised from a mature leaf from both drought-stressed and control plants of *A. helenae* and *A. vera* before and after the drought period and placed in 2-ml Eppendorf tubes in 100 µl 99.8% methanol (CH_3OH, 322415 Sigma-Aldrich, Merck, USA). Samples were frozen and stored at 20°C prior to investigation.

Transverse sections of approximately 3 mm in diameter were excised from the collected material and fixed for 30 min in 4% formaldehyde prepared from paraformaldehyde in phosphate-buffered saline (PBS). After two washes in PBS, sections were dehydrated in series of methanol:water solutions until reaching a final concentration of 100% methanol. The methanol was substituted with methanol: London Resin (LR) white resin mixture (1:1) for 8–10 hr and, finally, the sections were transferred to pure LR resin overnight. The specimens were placed and oriented in gelatine capsules filled with pure LR resin. The polymerization was performed in an oven at 60°C overnight. An ultramicrotome (Leica EM-UC7) was used to produce 1 µm-thick sections. These were adhered on Superfrost Slides (Thermo Scientific, Roskilde, Denmark) in a drop of water at 60°C.

Immunolocalization was performed as described by Mravec et al. (2017) using the antibodies LM21 and LM22 binding galactomannan or glucomannan (Marcus et al., 2010), BS-400-4 binding mannan (Pettolino et al., 2001), and CCRC-M170 binding acetylated mannan (Zhang et al., 2014) to understand the mannan distribution. In brief, leaf sections were placed on glass microscope slides, surrounded by a hydrophobic circle drawn with a PAP pen (Merck Life Science, Darmstadt, Germany), and blocked with 5% milk powder in PBS for 15 min. The leaf tissue was probed with antiglycan monoclonal antibodies for 1 hr at 1:10 dilution in 5% milk powder in PBS, washed two times with 5% milk powder in PBS, then probed with a secondary antibody. The secondary antibodies used were antirat or antimouse conjugated to Alexa Fluor 555 or Alexa Fluor 488 (Invitrogen) at 1:300 dilution in 3% bovine serum albumin in PBS. The leaf tissue was washed three times with PBS, counterstained with Calcofluor White (Sigma) at 0.1 mg/ml concentration for 10 min. Finally, the leaf tissue was washed once more and mounted in CitiFluor, an antifading reagent (Agar Scientific, Essex, United Kingdom).

The COS^{488} staining binding to deesterified homogalaturonan was performed as described by Mravec et al. (2014). "COS" stands for "chitosan oligosaccharides" in which the interaction between COS and homogalacturonan (HG) is governed by multiple polar interactions of protonated NH_2 on COS and carboxyl groups on demethyl esterified HG. COS recognizes HG with degree of esterification from 0 to approximately 38% (Mravec et al., 2014). Leaf sections were incubated with 1:1,000 COS^{488} (Mravec et al., 2014) and 0.1 mg/ml of Calcofluor White (Sigma) in 25-m 2-(N-morpholino)ethanesulfonic acid (MES) buffer for 30 min at room temperature. The leaf sections were then washed twice with MES buffer and mounted in MES:glycerol (1:1) solution.

Sections of *A. helenae* and *A. vera* were stained with 1% toluidine blue for 10 min to highlight all cell walls in the section, washed twice with distilled water, and mounted on glass slides under a coverslip. Images were taken on Olympus BX41 microscope with mounted Olympus ColorView I camera.

The fluorescently labelled samples were scanned using a Leica SP5 confocal laser scanning microscope equipped with UV diode (405 nm),

Ar (488 nm), and HeNe (543 nm) lasers at either 20× or 63× water objectives. The pictures were processed with GIMP2 software for colour enhancement and contrast. Control samples were treated equally.

For general comparative observations of leaf anatomy in a range of *Aloe* species, we used the extensive collection of permanent microscope slides located at the Royal Botanic Gardens, Kew. A Leica (Wetzlar, Germany) DM LB 100T light microscope was used to examine the prepared slides of leaf surfaces, transverse, and longitudinal sections; photomicrographs were taken using a Zeiss (Jena, Germany) AxioCam HRc mounted camera.

2.4 | Comprehensive microarray polymer profiling

The CoMPP analysis followed the protocol described by Ahl et al. (2018), optimized for succulent tissues from that of Moller et al. (2007). Hydrenchyma was carefully excised from mature harvested leaves of *A. helenae* and *A. vera* and immediately placed in labelled Falcon tubes (Corning, New York, USA) and snap frozen in liquid nitrogen. For each species, three samples were taken from three plants grown in individual pots. Samples were kept at −20°C for 24 hr before they were freeze dried. Three samples of approximately 5 mg were weighed to 1 decimal accuracy, and each placed in the well of an 8-strip tube (CLS4413 SIGMA, Merck Life Science, Darmstadt, Germany). The samples were homogenized in a Tissuelyser II (Gentec Biosciences, Columbia) using glass beads prior to extraction.

A three-step sequential extraction series was employed. For each sample, the extractant volume was adjusted to the exact weight of each sample. Glass beads were kept in the tubes to enhance mixing of tissues and solvents. For the first extraction step, dH_2O was added to dissolve all the soluble unbound or loosely bound polysaccharides. Samples were then shaken at room temperature for 27 s^{-1} for 2 min before the speed was reduced to 6 s^{-1} for 2 hr. After extraction, the samples were centrifuged at 4,000 RPM (Thermo-Fisher Scientific, Waltham, MA USA 02451) for 10 min, and the supernatant carefully removed and transferred to a labelled 0.5 -ml Eppendorf tube (Eppendorf AG, 22331 Hamburg, Germany). Extracts were stored at 5°C to minimize enzymatic or chemical change during the following extraction step. The precipitate pellet was retained for a subsequent extraction step.

In the second step, a 50-mM CDTA (trans-1,2-Diaminocyclohexane-*N*,*N*,*N*′,*N*′,-tetraacetic acid monohydrate, pH 7.5, 32869 SIGMA-ALDRICH, Merck Life Science, Darmstadt, Germany) was used following the same procedure as for dH_2O. Finally, 4-mM NaOH was added to the precipitate pellet for the last extraction, following the same procedure as for the previous two steps. When all samples were extracted, a four-fold serial dilution series was made for each sample and dilution in a 384-well microtiter plate (CLS3342 SIGMA Merck Life Science, Darmstadt, Germany). Extracts were diluted using Arrayjet buffer (55.2% glycerol, 44% water, and 0.8% Triton X-100), and the plate was centrifuged at 3,000 RPM (Thermo-Fisher Scientific, Waltham, MA USA 02451) for 10 min before samples were printed on a 0.45-μm nitrocellulose membrane (Whatman, Maidstone, UK) using an Arrayjet Sprint (Arrayjet Ltd., Edinburgh, UK) piezoelectric robotic printer. The dilution series were printed in duplicate on each microarray. As an earlier study observed problems with detection of mannans (Ahl et al., 2018), sample wait time between extraction and printing was minimized to prevent degradation and optimize quality of print following Ahl et al. (2019).

A total of 19 monoclonal antibodies were used for the microarray analyses as primary antibodies; the secondary antibodies (Merck Life Science, Darmstadt, Germany) were either antirat or antimouse depending on the primary antibody. The printed arrays were developed, quantified, and analysed following the procedures described by Ahl et al. (2018). A total of 62 arrays were used: one for each antibody in triplicates and two for negative controls of the secondary antibodies.

Averages were calculated using the dilution series for each sample and the array triplicates. The highest mean value of the dataset was assigned the value of 100%, and the remainder of the data was adjusted accordingly and normalized with a 5% cut off. The dataset is visualized in a heatmap format.

Species	Treatment	RWC (%)	SWC (%)
Aloe helenae	Drought stressed	43	30
Aloe helenae	Control	88	63
Aloe vera	Drought stressed	64	33
Aloe vera	Control	84	61

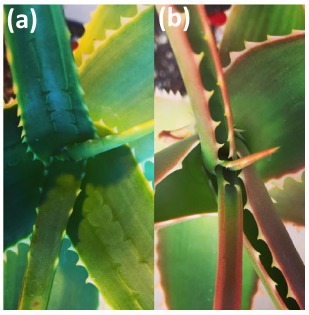

FIGURE 1 Effect of drought on two Aloe species. (table) The calculated relative and saturated water content for *Aloe helenae* and *Aloe vera* and measured before (control) and after 6 weeks of drought. *A. helenae* showed visible signs of drought stress. Pictures (a) and (b) show *A. helenae* (a) before and (b) after the drought period

3 | RESULTS

3.1 | RWC and SWC in *A. vera* and *A. helenae*

RWC and SWC were calculated for *A. helenae* and *A. vera* in both drought-stressed plants and well-watered control plants. Pronounced differences were seen in both species between the drought-stressed species and control plants (Figure 1). For both species, RWC of the control plants were consistently above 80%, whereas the drought-stressed plants were significantly reduced to below 65% for *A. vera* and as low as 43% for *A. helenae*. Similar differences were observed for the SWC, control species reaching above 60%, and the drought-stressed species being 33% for *A. vera* and 30% for *A. helenae*.

3.2 | In situ microscopy analysis of hydrenchyma cell walls in *A. vera* and *A. helenae*

Cell wall morphology of the hydrenchyma cells in watered and drought-stressed *A. helenae* and *A. vera* was investigated using microscopy (Figure 2). The leaves of *Aloe helenae* were longer, thinner, and

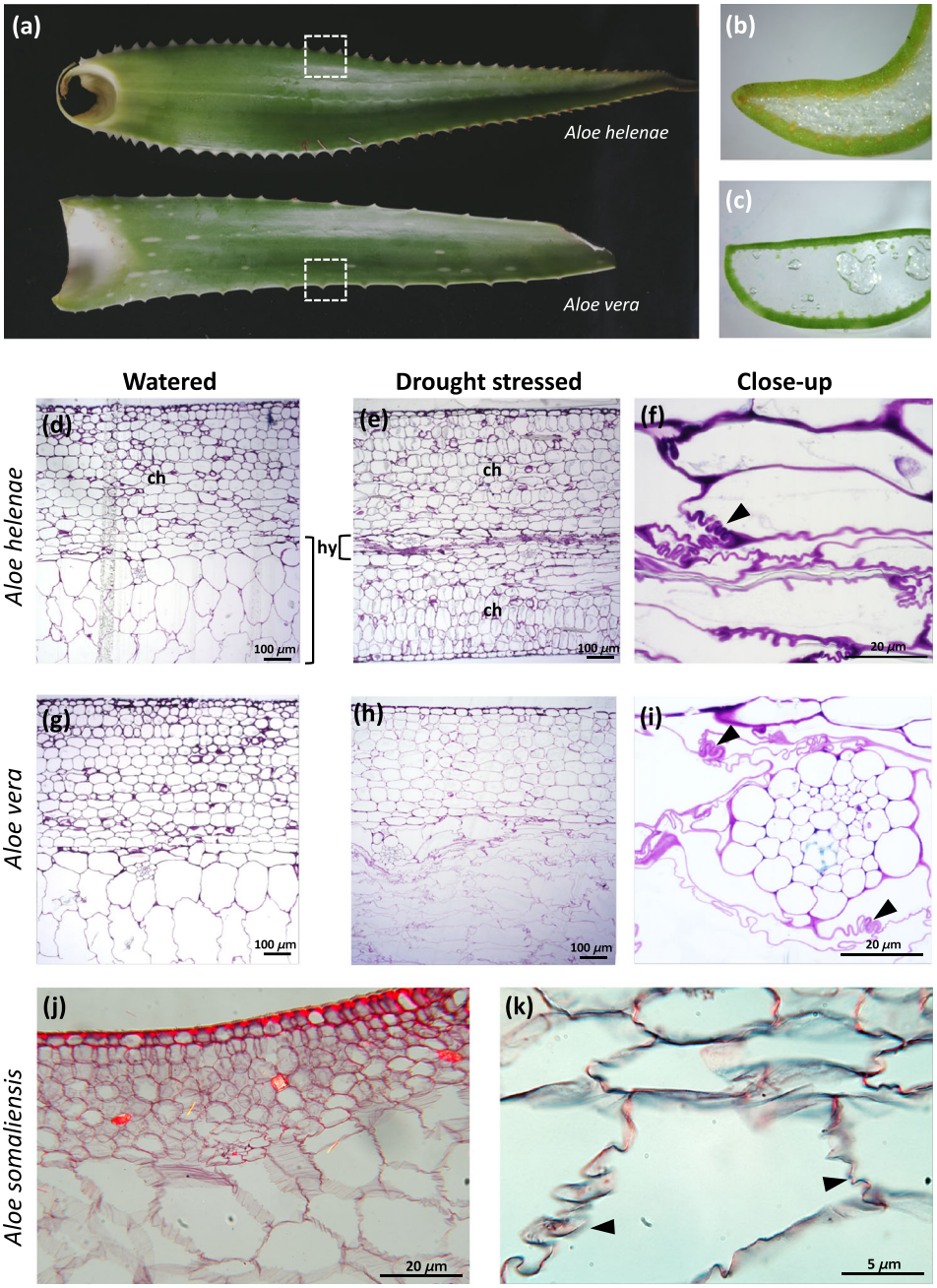

FIGURE 2 Comparative morphology and anatomy of *Aloe helenae* (a, b, d, e, and f), *Aloe vera* (a, c, g, h, and i), and *Aloe somaliensis* (j and k). Transverse sections (marked by dashed squares) of hydrenchyma tissue stained with toluidine blue showing typical leaf tissue arrangement in *Aloe* species with hydrenchyma, (h) surrounded by an outer photosynthetic chlorenchyma, (c) epidermis and cuticle (d, e, g and h). Convoluted folding of hydrenchyma cell walls in drought-stressed plants (f and i) indicated by arrows. *Aloe somaliensis* (j and k) from the Kew slide collection also showing folds in the hydrenchyma cell walls

the margins rolled inwards than those of *A. vera*. The epidermis of *A. helenae* was thicker than that of *A. vera*, whereas the hydrenchyma layer was thicker in *A. vera* than in *A. helenae* (Figure 2b,c). Based on the toluidine blue-stained micrographs, both species have chlorenchyma region composed of approximately 15 cell layer, whereas the thickness of hydrenchyma varied in both the watered and drought-stressed species (Figure 2d–i).

In *A. helenae*, the hydrenchyma had shrunk to a very thin layer after the plants had been exposed to drought (Figure 2e). In *A. vera*, shrinkage was less pronounced, but cell size and shape had changed: The hydrenchyma cells were transformed from uniformly rounded in hydrated samples to elongated and flat with uneven cell walls in drought-stressed samples (Figure 2g,h). In both species, the chlorenchyma was largely unaffected, and cell size was similar before and after drought.

In the drought-stressed plants (Figure 2f,i), the cell walls were pronouncedly convoluted, a type of folding where the cell wall does not collapse, but rather folds in regular patterns (Haberlandt, 1914). In some cells, the entire cell wall was continuously and moderately folded in a wavy or zig-zag pattern; otherwise, it was tightly folded several times in discontinuous regions of the wall (Figure 2f,i). Convoluted cell wall folding was observed in other species of *Aloe* represented in the permanent microscope slide collection of the Royal Botanic Gardens, Kew and illustrated here by *Aloe somaliensis*

(a)

			Pectins							Hemicelluloses					2°Ab control	
			Homogalacturonan					RG1		XG		Mannan			Negative	
Species	Extraction	Treatment	JIM5	JIM7	LM18	LM19	LM20	LM5	LM6	LM24	LM25	LM21	LM22	BS-400-4	Neg. R	Neg. M.
Aloe helenae	Water	Drought	0	0	0	0	0	0	0	0	0	32	0	30	0	0
Aloe helenae	Water	Watered	0	0	0	0	0	0	0	0	0	53	0	56	0	0
Aloe helenae	Water	Control	0	16	0	0	0	0	0	0	0	51	0	46	0	0
Aloe vera	Water	Drought	0	0	0	0	0	0	0	0	0	39	0	48	0	0
Aloe vera	Water	Watered	0	0	0	0	0	0	0	0	0	58	0	55	0	0
Aloe vera	Water	Control	0	20	0	0	0	0	0	0	0	56	0	70	0	0
Aloe helenae	CDTA	Drought	19	37	25	32	0	0	0	0	0	100	0	99	0	0
Aloe helenae	CDTA	Watered	0	5	5	0	5	0	0	0	0	50	0	57	0	0
Aloe helenae	CDTA	Control	0	0	9	6	0	0	0	0	0	69	0	69	0	0
Aloe vera	CDTA	Drought	0	0	0	0	0	0	0	0	0	52	0	56	0	0
Aloe vera	CDTA	Watered	0	0	0	0	0	0	0	0	0	41	0	47	0	0
Aloe vera	CDTA	Control	0	7	0	0	7	0	0	0	0	46	0	50	0	0
Aloe helenae	NaOH	Drought	0	0	0	0	0	0	0	0	28	50	0	72	0	0
Aloe helenae	NaOH	Watered	0	0	0	0	0	0	0	6	36	45	0	65	0	0
Aloe helenae	NaOH	Control	0	0	0	0	0	9	0	8	38	52	0	64	0	0
Aloe vera	NaOH	Drought	0	0	0	0	11	0	0	0	10	18	0	36	0	0
Aloe vera	NaOH	Watered	0	0	0	0	0	0	0	0	9	32	0	46	0	0
Aloe vera	NaOH	Control	0	0	0	0	0	0	0	0	11	20	0	42	0	0

(b)

			Pectins							Hemicelluloses					2°Ab control	
			Homogalacturonan					RG1		XG		Mannan			Negative	
Sample	Exctraction	Dilution	JIM5	JIM7	LM18	LM19	LM20	LM5	LM6	LM24	LM25	LM21	LM22	BS-400-4	Neg. R	Neg. M.
Aloe helenae	Combined	Drought	10	19	13	16	0	0	0	0	14	90	0	100	0	0
Aloe helenae	Combined	Watered	0	0	0	0	0	0	0	0	18	74	0	88	0	0
Aloe helenae	Combined	Control	0	11	0	0	0	7	0	0	19	85	0	89	0	0
Aloe vera	Combined	Drought	0	0	0	0	8	0	0	0	6	54	0	69	0	0
Aloe vera	Combined	Watered	0	0	0	0	0	0	0	0	5	66	0	74	0	0
Aloe vera	Combined	Control	0	14	0	0	0	0	0	0	6	60	0	80	0	0

Polymer	Code	Epitope	Origin	Data shown	Reference
Pectin	JIM5	HG with low DE	Rat	x	VandenBosch *et al.* 1989; Willats *et al.* 2000; Clausen *et al.* 2003
	JIM7	HG with high DE	Rat	x	VandenBosch *et al.* 1989; Willats *et al.* 2000; Clausen *et al.* 2003
	LM18	Partially methylesterified homogalactauronan	Rat	x	Verhertbruggen *et al.* 2009
	LM19	Partially methylesterified homogalactauronan	Rat	x	Verhertbruggen *et al.* 2009
	LM20	Partially methylesterified homogalactauronan	Rat	x	Verhertbruggen *et al.* 2009
	LM5	(1→4)-*β*-D-galactan	Rat	x	Jones *et al.* 1997
	LM6	(1→5)-*α*-L-arabinan	Rat	x	Willats *et al.* 1998; Lee *et al.* 2005; Verhertbruggen *et al.* 2009
	LM13	Linearised (1→5)-α-L-arabinan	Rat		Moller *et al.* 2008; Marcus *et al.* 2010
	LM16	6′-*β*-D-galactosyl-β-(1→4)-D-galactotriose	Rat		Verhertbruggen *et al.* 2009
Mannan	BS-400-4	(1→4)-*β*-D-mannan	Mouse	x	Pettolino *et al.* 2001
	LM21	(1→4)-*β*-D-mannan/galactomannan/glucomannan	Rat	x	Marcus *et al.* 2010
	LM22	(1→4)-*β*-D-mannan/galactomannan/glucomannan	Rat	x	Marcus *et al.* 2010
XG	LM24	Xyloglucan	Rat	x	Pedersen *et al.* 2012
	LM25	Xyloglucan	Rat	x	Pedersen *et al.* 2012
Xylan	LM10	(1→4)-*β*-D-xylan	Rat		McCartney *et al.* 2005
	LM11	(1→4)-*β*-D-xylan/arabinoxylan	Rat		McCartney *et al.* 2005
AGP	JIM8	AGP	Rat		McCabe et al. 1997
	JIM13	AGP	Rat		Knox *et al.* 1991; Yates *et al.* 1996
	JIM14	AGP, aldouronic acid	Rat		Knox *et al.* 1991; Yates *et al.* 1996

FIGURE 3 Heatmap representation of hydrenchyma polysaccharides of drought stressed, watered, and control treatments of *Aloe helenae* and *Aloe vera*: (a) all data from each extraction; (b) summed data from comprehensive microarray polymer profiling. Sums were made using the measured quantifications and are not the sums of the calculated data shown in (a). XG, xyloglucan; Ab, antibody; R, rat; M, mouse; RGI, rhamnogalacturonan-I. Data not shown here are available in the Supporting information

(Figure 2j,k). The watering scheme applied to the plants used to prepare permanent mounted slides in the slide collection was not recorded.

3.3 | CoMPP profiling of cell wall polysaccharides in response to drought

Compositional changes of *Aloe* polysaccharides in response to drought were detected using CoMPP. Of a total of 20 antibodies targeting different epitopes on the most common cell wall polysaccharides, only 10 gave a signal; a selection of these results is shown in Figure 3 (additional data in Figure S1 online). The strongest mannan signals (LM21 and BS-400-4) were observed in the CDTA extraction from both species. Only two of the mannan specific antibodies (LM21 and BS-400-4) detected epitopes in both *A. vera* and *A. helenae* in all three extraction steps; both detecting more in *A. helenae* than *A. vera* in all extractions.

The most noticeable differences between the polysaccharide composition of drought-stressed and watered control samples were observed in *A. helenae* in the CDTA extraction, which contained very low pectin levels as seen by the homogalacturonan detected by the antibodies JIM5, JIM7, LM18, and LM19 (Clausen, Willats, & Knox, 2003; Vandenbosch et al., 1989; Verhertbruggen, Marcus, Haeger, Ordaz-Ortiz, & Knox, 2009; Willats et al., 2000). However, in the drought-stressed samples, the signals were strong even for antibodies that showed no detection in the watered and control samples. A similar pattern was observed for the mannan-specific antibodies LM21 and BS-400-4, for which signal strengths were almost double in the CDTA extraction of *A. helenae*. Drought also increased pectin signal in *A. helenae*, although the pectin specific antibody LM20 gave a weak response. No pectin signals were seen for *A. vera* in the water and CDTA extractions, yet a very vague LM20 signal appeared in drought-stressed *A. vera* in the NaOH extraction. *A. vera* also showed differences in the mannan signals between the watered and drought-stressed plants in all extractions but were relatively weakly compared with *A. helenae*.

No signals were detected for the antibodies targeting xylan (LM10 and LM11) and only very little AGP (JIM8, JIM13, and Jim14; Knox, Linstead, Cooper, & Roberts, 1991; McCabe, Valentine, Forsberg, & Pennell, 1997; McCartney, Marcus, & Knox, 2005; Pedersen et al., 2012; Yates et al., 1996). Likewise, only sporadic signals were

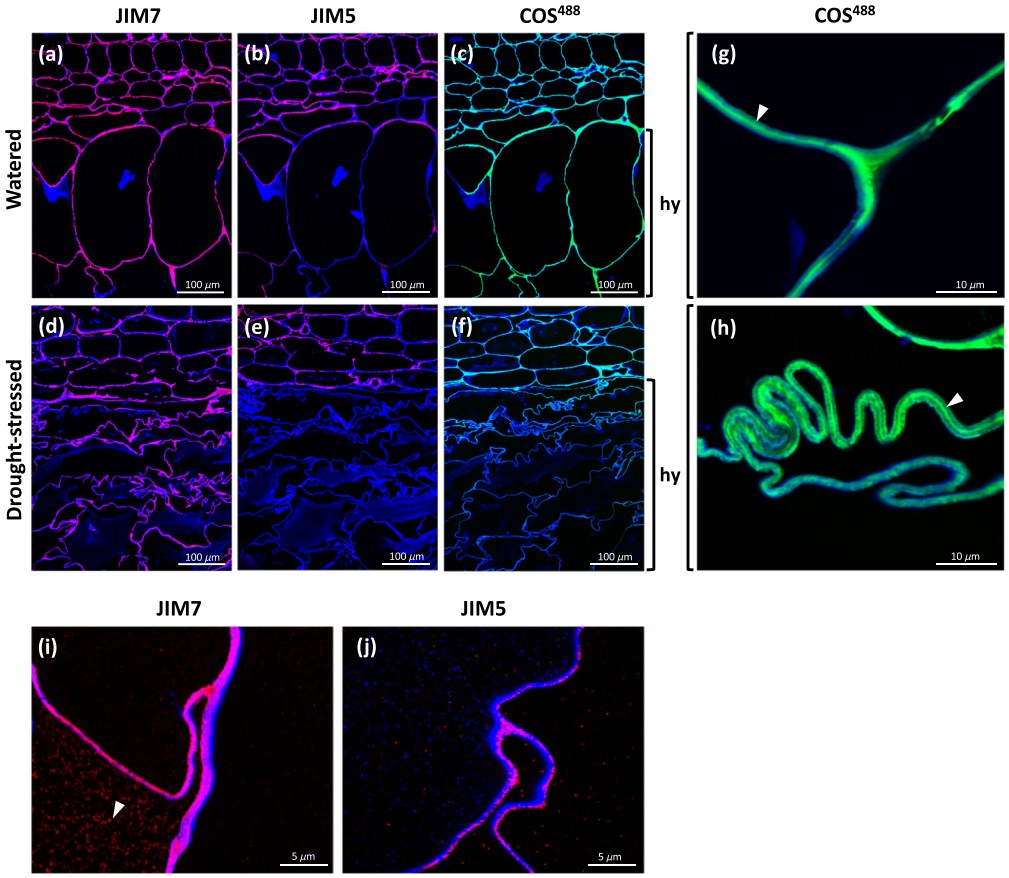

FIGURE 4 In situ detection of homogalacturonan in sections of *Aloe vera* leaves using monoclonal antibodies JIM7 (binding highly methylated homogalacturonan), JIM5 (binding homogalacturonan with a low degree of esterification), and COS488 (binding highly deesterified homogalacturonan); images overlayed with Calcofluor White signal (blue) highlighting the cell walls. Micrographs showing (a–c) watered and (d–f) drought-stressed specimens show remarkable changes in cell wall polysaccharide composition and folding. Detail is shown in (g–j) high magnification micrographs. Arrowheads indicate (g and h) middle lamella and (i) intracellular accumulation

detected from the RG-I specific antibodies (LM5, LM6, LM13, and LM16; Lee et al., 2005; Moller et al., 2008; Willats, Marcus, & Knox, 1998). Data shown in the Supporting information online.

3.4 | Distribution of structural polysaccharides in hydrenchyma cell walls and intracellular compartments

To further understand the mechanism behind the cell wall folding, we investigated the composition of the hydrenchyma cell walls in situ (Figure 4). We analysed the presence of homogalacturonan as the main pectic component and one of the crucial determinants of cell wall mechanical properties. Both immunological and nonimmunological probes were used: The oligosaccharide probe COS^{488}, staining longer stretches of deesterified homogalacturonan (Mravec et al., 2014), and JIM5 and JIM7, recognizing homogalacturonan with a low or high level of deesterification, respectively (Clausen et al., 2003; Vandenbosch et al., 1989; Willats et al., 2000; Figure 4). In *A. vera* (Figure 4a–f), the JIM5 signal was restricted to the chlorenchyma cell walls and gave only a weak and sporadic signal in the hydrenchyma cell walls, especially at the triangular junctions. In contrast, JIM7 gave a strong signal throughout the leaf section and was unaffected by drought. In the drought-stressed specimens, the signal for JIM5 disappeared from the shrunken hydrenchyma. COS^{488} gave a strong signal in all cell walls in the control sample. However, in the drought-stressed specimen, the signals for JIM5 and COS^{488} were noticeably reduced in hydrenchyma. This effect was also clearly seen in *A. helenae* (Figure S2). When examined in higher magnification (Figure 4g–j), none of the immunological probes gave middle lamellar and cell corner staining typical of other parenchymatic tissues. The JIM7 signal also appeared inside the cells as distinct compartments different to those stained with Calcofluor White (Figure 4i). Instances of middle lamella staining were sporadically observed only for COS^{488} (Figure 4g,h).

We also investigated the distribution of other pectin types. Immunolocalization showed no appreciable labelling with either LM5 (binding (1,4)-β-D-galactan) or LM6 (binding (1,5)-α-L-arabinan) monoclonal antibodies (Figure S3), suggesting cell walls in hydrenchyma are low in RG-I side chains (Jones, Seymour, & Knox, 1997; Lee et al., 2005; Verhertbruggen et al., 2009; Willats et al., 1998). We also tested the presence of other cell wall components for which antibodies were available: Relatively small amounts of xyloglucan (using LM15) were detected, but other polysaccharides and proteoglycans (extensins, AGPs) were almost completely absent when probed on sections (data not shown). These observations would be in line with CoMPP results indicating that the cell walls of hydrenchyma are formed mainly with mannan, xyloglucan, and homogalacturonan out of the polysaccharides that we measured for. The hydrenchyma cell walls are thus lacking some of the compositional complexity seen in other primary cell wall types found in other organs (Fangel et al., 2012).

3.5 | In situ distribution of *Aloe* mannans

To analyse the distribution of acetylated mannan and its molecular variants in situ and immunolocalization on LR-resin, sections were made using the same set of antimannan antibodies as for CoMPP with the addition of CCRC-M170. The immunolocalization showed mannan widely distributed in the entire cross-section and not exclusively in hydrenchyma and could be seen as associated with the cell wall and as patchy populations of granular intracellular signals (Figures 5 and 6). The binding of BS-400-4 and to a lesser extent LM21 was

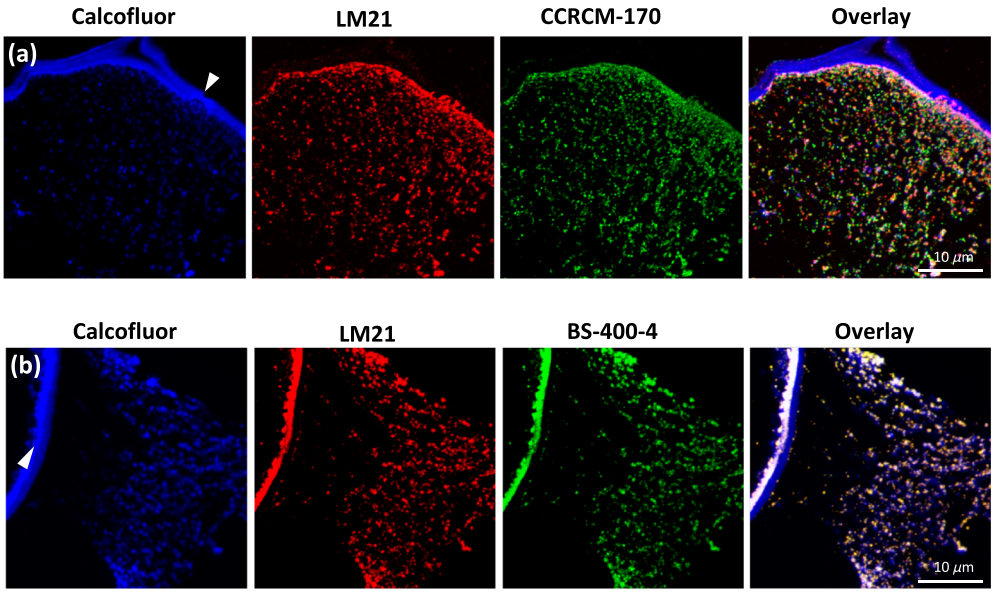

FIGURE 5 In situ detection of mannan epitopes in *Aloe vera* hydrenchyma using three monoclonal antibody probes. (a) Colocalization of Calcofluor White (blue signal), LM21 (red signal) recognizing β-(1,4)-mannan/galactomannan/glucomannan, and CCRCM-170 (green signal) recognizing acetylated mannan; (b) colocalization of Calcofluor White (blue signal), LM21 (red signal), and BS-400-4 recognizing β-(1,4)-galactomannan (green signal); cell wall is marked with arrowheads

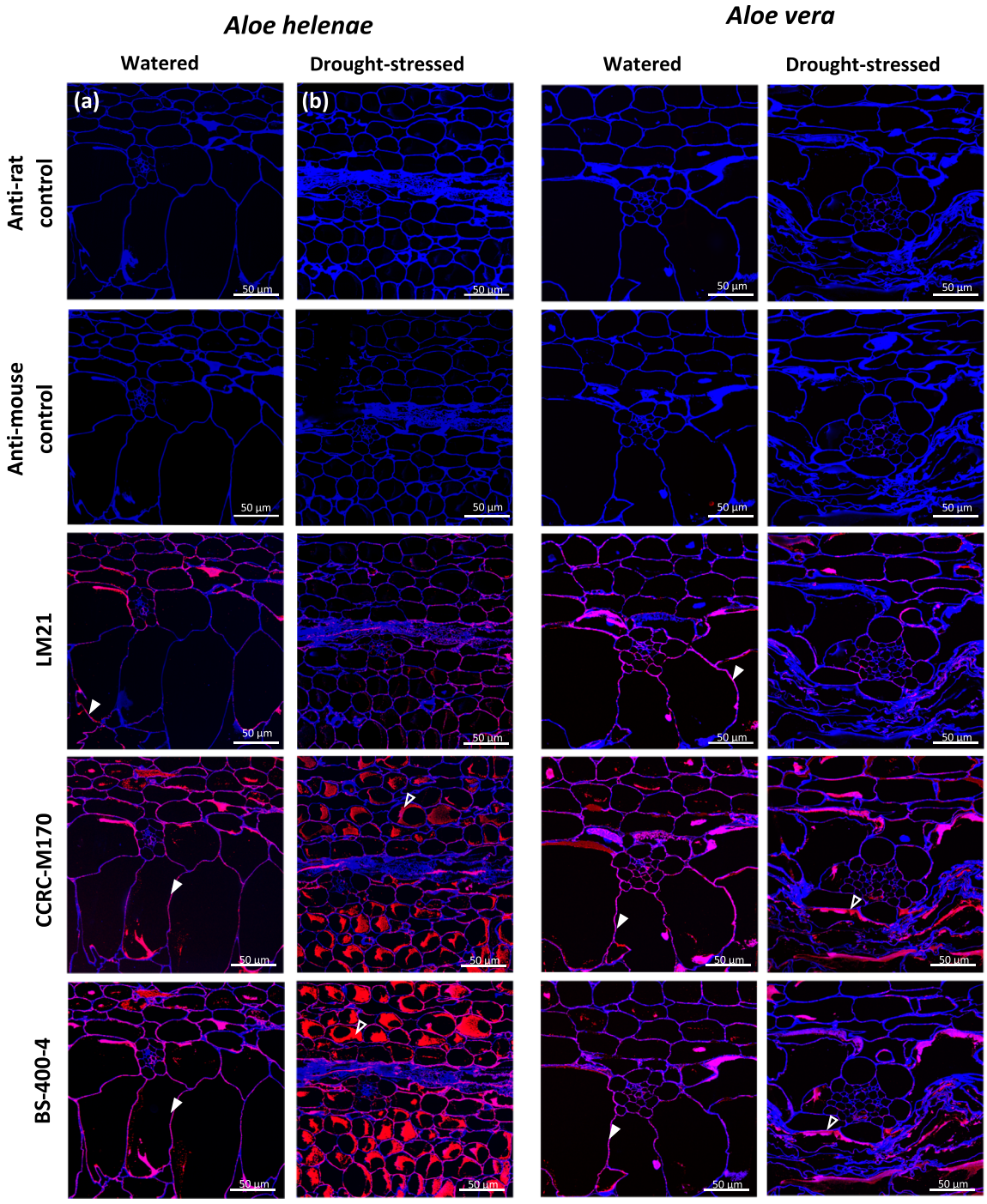

FIGURE 6 Detection of mannan using three different antimannan monoclonal antibodies on sections of *Aloe helenae* (a, b) and *Aloe vera* (c, d) hydrenchyma in (a, c) well-watered, and (b,\c) drought-stressed samples. LM21 binds (1,4)-β-D-mannan/galactomannan/glucomannan, CCRCM170 binds acetylated mannan, and BS-400-4 binds (1,4)-β-D-mannan. Calcofluor White (staining β-(1,4) glucans) is used on all sections. The cell wall signal is marked by closed arrowhead and the intracellular signal with open arrowheads

enhanced by pretreatment with 200-mM NaOH in all leaf tissues, confirming that the epitopes recognized by LM21 are partially masked by the acetylations (Figure S4). The CCRC-M170 antibody also showed the distribution of mannan throughout the cross-section of a leaf, whereas the pretreatment with 200-mM NaOH diminished the signal, hence confirming the requirement of acetylation for the CCRC-M170 recognition (Figure S4). The close inspection of the sections probed with anti-mannan monoclonal antibodies revealed that all mannan epitopes could be seen as bead-like round compartments 0.1–1 µm in size. These compartments were also observed by in vivo labelling of tissue streaks using Vectabond slides, confirming that they are not an embedding artefact (Figure S5).

The colabelling using CCRC-M170 and LM21 showed only partial overlay (Figure 5a) whereas the colocalization using LM21 and BS-

400-4 showed a near-complete match (Figure 5b). These patterns suggest some intramolecular structural heterogeneity of *Aloe* mannan polymers and their intracellular distribution in relation to their acetylation (Figure 5). Furthermore, Calcofluor White, a specific dye for β–(1,4)-glucan, stained similar sized compartments yet only partial colocalization was detected, indicating the presence of other compartments possibly filled by nonmannan types of β-glucans (Figure 5). We found that the stressed plants of *A. helenae* and *A. vera* gave a lower mannan signal in shrunken hydrenchyma, not only particularly CCRC-M170 but also partially by LM21 (Figures 6 and 7). In watered plants, the mannan compartments were mainly associated with the cell wall or distributed around the borders of the cells, probably pushed toward the cell wall by the central vacuole yet were more dispersed within the cell in drought stressed, which could be an effect of the shrinkage of the central vacuole.

4 | DISCUSSION

4.1 | Convoluted folding of cell walls provides a structured response to drought

Our findings highlight the ecological significance of a somewhat overlooked anatomical feature of hydrenchyma tissue: cell wall convolution as a regulated structural response to drought. Convoluted cell walls were initially reported in *Aloe* by Pfizer (Haberlandt, 1914), but have since received little attention as a morphological trait associated with succulence (but see an example of *Aloe pearsonii* in von Willert, Eller, Werger, Brinckmann, and Ihlenfeldt [1992]). The regular folding mechanism is a necessary measure to reduce cell size during dehydration without shrinking or altering the cell wall (Haberlandt, 1914), which could otherwise result in costly cell loss or repair during

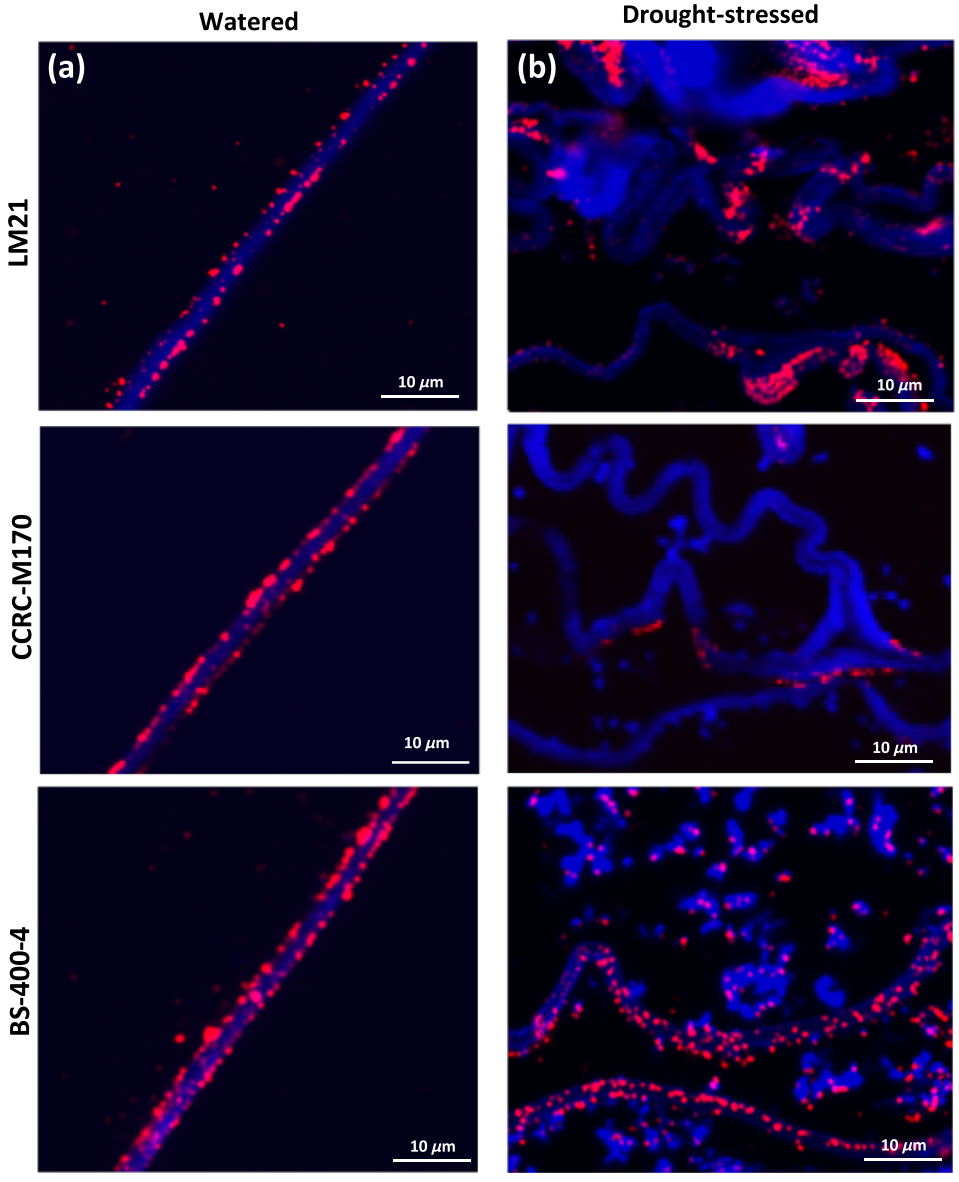

FIGURE 7 Changes in cell wall-associated mannan in watered and droughtstressed leaf hydrenchyma tissue of *Aloe helenae*. The sections are probed with LM21, CCRC-M170, and BS-400-4 in (a) watered and (b) drought-stressed specimens. Note the disappearance of the CCRCM-170 and partial disappearance of LM21 in hydrenchyma of drought-stressed specimen

postdrought recovery. Cell wall folding has also been postulated to influence the shape and position of the dehydrated leaf on the plant, minimizing temperature and radiation damage under drought conditions (von Willert et al., 1992).

Our observations indicate that the reduction in the volume of water-storing hydrenchyma in *Aloe* during drought is not caused by random cell collapse but represents a closely regulated and controlled process in which cell wall folding allows desiccated hydrenchyma cells to retain the potential to unfold subsequently by isotropic expansion of the cell. The folding of hydrenchyma cell walls occurs more frequently in drought-stressed plants but may be a more general mechanism for regulating leaf shape in *Aloe* in response to less severe fluctuations in water availability. Our results pinpoint homogalacturonan and its esterification in the folding process. The distribution of different types of homogalacturonan in hydrenchyma and chlorenchyma changes under drought and watered conditions with drought-stress-induced loss of homogalacturonan with low degrees of esterification, whereas homogalacturonan with a high degree of esterification was largely unaffected. We postulate that the loss of deesterified homogalacturonan available for Ca^{2+}-mediated complexation might release the internal constrains within the cell wall, triggering the folding response. It would be interesting to study the enzymatic mechanisms underlying this homogalacturonan dynamics in the future (Saffer, 2018).

Drought-stressed plants of *A. helenae* and *A. vera* differed significantly in RWC and SWC. Despite the resilience imparted by cell walls, drought stress events negatively impact the capacity of hydrenchyma to fully rehydrate following a drought event. Prior to sampling, *A. helenae* appeared to be more negatively affected by drought than *A. vera* (Figure 1) with red-coloured leaves, loss of turgidity, and in-rolled margins. Interestingly, *A. helenae* showed higher RWC and SWC in the control plants, indicating a more rapid cellular response to drought compared with *A. vera*.

The observed variation in water content storage ability and flexibility could reflect habitat-specific adaptations, and the differences in response time might also be linked to unique polysaccharide composition of the cell walls for each species.

4.2 | Cell wall polysaccharides with flexibility and storage functions dominate in *Aloe*

The composition of structural *Aloe* polysaccharides and the lack of components related to the mechanisms of cell wall extensibility and rigidity (e.g., galactans) are consistent with the requirement for high flexibility to accommodate cell wall folding. Indeed, acetylated mannan and galacto (gluco)mannan were the most frequently detected polysaccharides in both the microscopy and the CoMPP analysis of *Aloe* hydrenchyma (Figures 3 and 5). It has been suggested that acetylated mannan is involved in water storage in epiphytic orchids (Stancato et al., 2001). In *Aloe*, the abundance of mannan in the hydrenchyma cell walls of both *A. helenae* and *A. vera* would indicate that this polysaccharide is, likewise, implicated in water storage (Figures 5 and 7). The main hemicellulosic components detected in the cell walls of *Aloe* hydrenchyma were different types of homopolymers of mannan, galactomannans or glucomannans, and in lower amounts xyloglucan (Figure 4). The cellulose content requires an extraction step using cadoxen (Moller et al., 2007), and due to its corrosiveness and toxicity, is usually avoided and cellulose content excluded from CoMPP measurements. However, other studies have already confirmed the presence of cellulose in *Aloe* parenchymatous tissue (Femenia, Sanchez, Simal, & Rossell, 1999; Ni, Turner, Yates, & Tizard, 2004; Rodríguez-González et al., 2011). This was supported by the Calcofluor White staining in the present study.

Antibody detection of mannan in tissue sections (Figure 5) revealed that different epitopes of mannan are stored separately in distinct intracellular compartments and have a granular appearance as opposed to the more continuous distribution when it is embedded in the cell wall. The granular form of mannan resembles that of starch, a well-known storage polysaccharide. This observation provides further support for the hypothesis that mannan plays a role in energy storage and offers a source of carbohydrates for photosynthesis and maintaining water potential gradients between the chlorenchyma and hydrenchyma during drought conditions (Kluge & Ting, 1978; Nobel, 2006; Surridge, 2019). The precise nature and role of the granules that we identify in this study require further investigation to explore whether this is a common mechanism in succulent plants. That there is a link between polysaccharides and CAM has previously been shown (Kluge & Ting, 1978; Reynolds, 2004), and with the high content of mannan detected in aloes, it seems plausible that the two could be linked and thus enhance the survivability of succulents in extreme conditions. Future studies to resolve the biosynthetic pathway of mannan, the role of the mannan-containing granules and the polysaccharides connection to CAM will improve our understanding of how these two systems interact to improve the resilience of *Aloe* to drought.

4.3 | Cell wall polysaccharide composition changes in response to drought

Remobilization of polysaccharides and organized cell wall folds are recognized in the hydrenchyma tissue of drought-stressed *Aloe* species. Our findings indicate the involvement of mannans in relation to water storage, but the size of the response (increase or decrease) and direction (up or down regulation) may differ between species. As seen for *A. helenae*, the total mannan and pectin levels increased after drought, whereas the opposite (to a lesser degree) was true for *A. vera* (Figure 3b). The detection of polysaccharides using CoMPP may be influenced by their extractability (for instance, partial digestion during remobilization), suggesting that further investigations are needed to explore this phenomenon and how it may affect the total level of mannan. This methodological limitation also necessitates micromorphological analysis using monoclonal antibodies.

Minor differences between the watered and the control measurements in CoMPP are also likely due to natural fluctuations (Ahl et al.,

2019). The changes between predrought- and drought-stressed specimens were found for both species, although not in the same polysaccharide structures (Figure 3). Follow up studies are likely to illuminate species-specific drought tolerance in *Aloe* species, given that in this study *A. helenae* appeared to be more severely drought stressed than *A. vera* (Figure 1). The role of changing polysaccharide composition in drought recovery and resilience and the water-storing capacity of hydrenchyma tissue also require further consideration.

Considerable diversity in succulence between *Aloe* species likely reflects adaptations to varied habitats (Grace et al., 2015). The global popularity of *A. vera* is also attributed to its high polysaccharide content (Ahl et al., 2018; Eberendu et al., 2005; Shi et al., 2017). Therefore, predictable changes in the polysaccharide composition of *Aloe* species stimulated by drought stress or water availability could have practical ramifications for the management of species farmed for the hydrenchyma tissue, such as *Aloe arborescence* in Asia, *A. vera* on the American subcontinents, and *A. ferox* in South Africa (Grace, 2011).

Cell wall polysaccharides in *Aloe* are of ecological and economic significance in drought tolerance. We conclude that convoluted cell wall folding allows for controlled shrinking of dehydrated hydrenchyma and subsequent unfolding postdrought, although this process is not straightforward and the tissue may not recover its previous capacity for water storage. The most ubiquitous cell wall polysaccharides in *Aloe* appear to be different forms of mannan. Drought-induced changes to the polysaccharide composition of *Aloe* hydrenchyma impact mannan abundance in particular, and these shifts could have implications for the commercial production of *A. vera* and other species.

ACKNOWLEDGMENTS

We thank horticulturist Martin Årseth-Hansen (Botanical Garden, Natural History Museum of Denmark) for providing plant material, Jeanett Hansen for help in the laboratory at PLEN, and Henriette L. Pedersen for discussion of CoMPP methods and results. The research was supported by grants from the Villum Foundation (Planet Project 9283) and the Carlsberg Foundation (grant CF17-0181).

CONFLICT OF INTEREST

The authors declare that they have no conflict of interest.

AUTHOR CONTRIBUTIONS

L. I. A. and J. M. conceived and designed the experiments with O. M. G. and P. J. R. L. I. A. conducted the CoMPP experiments. J. M. conducted the microscopy imaging. O. M. G. and P. J. R. contributed micrographs from the permanent slide collection at the Royal Botanic Gardens, Kew. L. I. A. and J. M. wrote the manuscript with the assistance of N. R. and O. M. G. All authors contributed to the analysis and discussion of the results and edited the manuscript.

FUNDING INFORMATION

Research grant from the Villum Foundation, Denmark, Planet Project 9283 (B. J., L. I. A., N. R.) and 17489 (J. M.).

ORCID

Louise Isager Ahl https://orcid.org/0000-0002-4727-1882
Jozef Mravec https://orcid.org/0000-0003-0331-3304
Bodil Jørgensen https://orcid.org/0000-0002-0453-1277
Paula J. Rudall https://orcid.org/0000-0002-4816-1212
Nina Rønsted https://orcid.org/0000-0002-2002-5809
Olwen M. Grace https://orcid.org/0000-0003-1431-2761

REFERENCES

Ahl, L. I., Al-Husseini, N., Al-Helle, S., Staerk, D., Grace, O. M., Mravec, J., … Rønsted, N. (2019). Detection of seasonal variation in Aloe polysaccharides using carbohydrate microarray polymer profiling. *Frontiers in Plant Science*, *10*, 512. **(Submitted)**

Ahl, L. I., Grace, O. M., Pedersen, H. L., Willats, W. G. T., Jørgensen, B., & Rønsted, N. (2018). Analyses of Aloe polysaccharides using carbohydrate microarray profiling. *Journal of AOAC International*, *101*, 1711–1719.

Albersheim, P., Darvill, A., Roberts, K., Sederoff, R., & Staehelin, A. (2011). *Plant cell walls: From chemistry to biology*. New York: Garland Science.

Beaumont, J., Cutler, D. F., Reynolds, T., & Vaughan, J. G. (1985). The secretory tissue of aloes and their allies. *Israel Journal of Botany*, *34*, 265–282.

Becker, B. (2007). Function and evolution of the vacuolar compartment in green algae and land plants (Viridiplantae). *International Review of Cytology*, *264*, 1–24. https://doi.org/10.1016/S0074-7696(07)64001-7

Buckeridge, M. S. (2010). Seed cell wall storage polysaccharides: Models to understand cell wall biosynthesis and degradation. *Plant Physiology*, *154*, 1017–1023. https://doi.org/10.1104/pp.110.158642

Chauhan, P. S., Puri, N., Sharma, P., & Gupta, N. (2012). Mannanases: Microbial sources, production, properties and potential biotechnological applications. *Applied Microbiology and Biotechnology*, *93*, 1817–1830. https://doi.org/10.1007/s00253-012-3887-5

Clausen, M. H., Willats, W. G. T., & Knox, J. P. (2003). Synthetic methyl hexagalacturonate hapten inhibitors of anti-homogalacturonan monoclonal antibodies LM7, JIM5 and JIM7. *Carbohydrate Research*, *338*, 1797–1800. https://doi.org/10.1016/S0008-6215(03)00272-6

Cosgrove, D. J. (2005). Growth of the plant cell wall. *Nature Reviews Molecular Cell Biology*, *6*, 850–861. https://doi.org/10.1038/nrm1746

Cosgrove, D. J. (2016). Plant cell wall extensibility: Connecting plant cell growth with cell wall structure, mechanics, and the action of wall-modifying enzymes. *Journal of Experimental Botany*, *67*, 463–476. https://doi.org/10.1093/jxb/erv511

Eberendu, A. R., Luta, G., Edwards, J. A., Mcanalley, B. H., Davis, B., Rodriguez, S., & Ray Henry, C. (2005). Quantitative colorimetric analysis of aloe polysaccharides as a measure of *Aloe vera* quality in commercial products. *Journal of AOAC International*, *88*, 684–691.

Fangel, J. U., Pedersen, H. L., Melgosa, S. V., Ahl, L. I., Salmean, A. A., Egelund, J., … Willats, W. G. T. (2012). Carbohydrate microarrays in plant science. *Methods in Molecular Biology*, *918*, 351–362. https://doi.org/10.1007/978-1-61779-995-2_19

Femenia, A., Sanchez, E. S., Simal, S., & Rossell, C. (1999). Compositional features of polysaccharides from *Aloe vera* (*Aloe barbadensis* Miller) plant tissues. *Carbohydrate Polymers*, *39*, 109–117. https://doi.org/10.1016/S0144-8617(98)00163-5

Grace, O. M. (2011). Current perspectives on the economic botany of the genus *Aloe* L. (Xanthorrhoeaceae). *South African Journal of Botany*, *77*, 980–987. https://doi.org/10.1016/j.sajb.2011.07.002

Grace, O. M. (2019). Succulent plants as natural capital. *Plants People Planet*, *00*, 1–10.

Grace, O. M., Buerki, S., Symonds, M. R., Forest, F., van Wyk, A. E., Smith, G. F., … Rønsted, N. (2015). Evolutionary history and leaf succulence as explanations for medicinal use in aloes and the global popularity of Aloe vera. *BMC Evolutionary Biology*, *15*, 29. https://doi.org/10.1186/s12862-015-0291-7

Haberlandt, G. (1914). *Physiological plant anatomy* (4th ed.). London: Macmilland and co.

Jones, L., Seymour, G. B., & Knox, J. P. (1997). Localization of pectic galactan in tomato cell walls using a monoclonal antibody specific to (1-4)-[beta]-D-galactan. *Plant Physiology*, *113*, 1405–1412. https://doi.org/10.1104/pp.113.4.1405

Kluge, M., & Ting, I. P. (1978). *Crassulacean acid metabolism*. Berlin, Heidelberg: Springer-Verlag. https://doi.org/10.1007/978-3-642-67038-1

Knox, J. P., Linstead, P. J., Cooper, J. P. C., & Roberts, K. (1991). Developmentally regulated epitopes of cell surface arabinogalactan proteins and their relation to root tissue pattern formation. *The Plant Journal*, *1*, 317–326. https://doi.org/10.1046/j.1365-313X.1991.t01-9-00999.x

Lambers, H., Chapin, F. S. III, & Pons, T. L. (1998). *Plant physiological ecology* (1st ed.). New York: Springer-Verlag. https://doi.org/10.1007/978-1-4757-2855-2

Landrum, J. V. (2002). Four succulent families and 40 million years of evolution and adaptation to xeric environments: What can stem and leaf anatomical characters tell us about their phylogeny? *Taxon*, *51*, 463–473. https://doi.org/10.2307/1555064

Lee, K. J. D., Sakata, Y., Mau, S., Pettolino, F., Bacic, A., Quatrano, R. S., … Knox, J. P. (2005). Arabinogalactan proteins are required for apical cell extension in the moss *Physcomitrella patens*. *Plant Cell*, *17*, 105–105.

Males, J. (2017). Secrets of succulence. *Journal of Experimental Botany*, *68*, 2121–2134. https://doi.org/10.1093/jxb/erx096

Marcus, S. E., Blake, A. W., Benians, T. A. S., Lee, K. J. D., Poyser, C., Donaldson, L., … Knox, J. P. (2010). Restricted access of proteins to mannan polysaccharides in intact plant cell walls. *Plant Journal*, *64*, 191–203. https://doi.org/10.1111/j.1365-313X.2010.04319.x

McCabe, P. F., Valentine, T. A., Forsberg, L. S., & Pennell, R. I. (1997). Soluble signals from cells identified at the cell wall establish a developmental pathway in carrot. *The Plant Cell Online*, *9*, 2225–2241. https://doi.org/10.1105/tpc.9.12.2225

McCartney, L., Marcus, S. E., & Knox, J. P. (2005). Monoclonal antibodies to plant cell wall xylans and arabinoxylans. *Journal of Histochemistry and Cytochemistry*, *53*, 543–546. https://doi.org/10.1369/jhc.4B6578.2005

Moller, I., Marcus, S. E., Haeger, A., Verhertbruggen, Y., Verhoef, R., Schols, H., … Willats, W. (2008). High-throughput screening of monoclonal antibodies against plant cell wall glycans by hierarchical clustering of their carbohydrate microarray binding profiles. *Glycoconjugate Journal*, *25*, 37–48. https://doi.org/10.1007/s10719-007-9059-7

Moller, I., Sørensen, I., Bernal, A. J., Blaukopf, C., Lee, K., Øbro, J., … Willats, W. G. (2007). High-throughput mapping of cell-wall polymers within and between plants using novel microarrays. *Plant Journal*, *50*, 1118–1128. https://doi.org/10.1111/j.1365-313X.2007.03114.x

Moore, J. P., Vicré-Gibouin, M., Farrant, J. M., & Driouich, A. (2008). Adaptations of higher plant cell walls to water loss: Drought vs desiccation. *Physiologia Plantarum*, *134*, 237–245. https://doi.org/10.1111/j.1399-3054.2008.01134.x

Mravec, J., Kracun, S. K., Rydahl, M. G., Westereng, B., Miart, F., Clausen, M. H., … Willats, W. G. (2014). Tracking developmentally regulated post-synthetic processing of homogalacturonan and chitin using reciprocal oligosaccharide probes. *Development*, *141*, 4841–4850. https://doi.org/10.1242/dev.113365

Mravec, J., Kračun, S. K., Rydahl, M. G., Westereng, B., Pontiggia, D., De Lorenzo, G., … Willats, W. G. T. (2017). An oligogalacturonide-derived molecular probe demonstrates the dynamics of calcium-mediated pectin complexation in cell walls of tip-growing structures. *Plant Journal*, *91*, 534–546. https://doi.org/10.1111/tpj.13574

Ni, Y., Turner, D., Yates, K. M., & Tizard, I. (2004). Isolation and characterization of structural components of *Aloe vera* L. leaf pulp. *International Immunopharmacology*, *4*, 1745–1755. https://doi.org/10.1016/j.intimp.2004.07.006

Nobel, P. S. (2006). Parenchyma-chlorenchyma water movement during drought for the hemiepiphytic cactus *Hylocereus undatus*. *Annals of Botany*, *97*, 469–474. https://doi.org/10.1093/aob/mcj054

Nyffeler, U., & Eggli, R. (2009). Living under temporarily arid conditions-succulence as an adaptive strategy. *Bradleya*, *27*, 13–36.

Ogburn, R. M., & Edwards, E. J. (2010). Chapter 4—The ecological water-use strategies of succulent plants. *Advances in Botanical Research*, *55*, 179–225. https://doi.org/10.1016/B978-0-12-380868-4.00004-1

Ogburn, R. M., & Edwards, E. J. (2012). Quantifying succulence: A rapid, physiologically meaningful metric of plant water storage. *Plant, Cell & Environment*, *35*, 1533–1542. https://doi.org/10.1111/j.1365-3040.2012.02503.x

Paulsen, B. S., & Barsett, H. (2005). Bioactive pectic polysaccharides. In T. Heinze (Ed.), *Polysaccharides 1: Advances in polymer science* (p. 186). Berlin, Heidelberg: Springer.

Pauly, M., Gille, S., Liu, L., Mansoori, N., de Souza, A., Schultink, A., & Xiong, G. (2013). Hemicellulose biosynthesis. *Planta*, *238*, 627–642. https://doi.org/10.1007/s00425-013-1921-1

Pedersen, H. L., Fangel, J. U., McCleary, B., Ruzanski, C., Rydahl, M. G., Ralet, M.-C., … Willats, W. G. (2012). Versatile high resolution oligosaccharide microarrays for plant glycobiology and cell wall research. *The Journal of Biological Chemistry*, *287*, 39429–39438. https://doi.org/10.1074/jbc.M112.396598

Pettolino, F. A., Hoogenraad, N. J., Ferguson, C., Bacic, A., Johnson, E., & Stone, B. A. (2001). A (1-4)-beta-mannan-specific monoclonal antibody and its use in the immunocytochemical location of galactomannans. *Planta*, *214*, 235–242. https://doi.org/10.1007/s004250100606

Pfitzer, E. (1877). Bemerkungen über die Wasseraufnahme abgeschnittener Pflanzenteile. *Verhandlungen des Naturhistorisch-Medizinischen Vereins zu Heidelberg*, *NF1*, 503–508.

Pimienta-Barrios, E., González, D., Castillo-Aranda, M. E., & Nobel, P. S. (2002). Ecophysiology of a wild *Platyopuntia* exposed to prolonged drought. *Environmental and Experimental Botany*, *47*, 77–86. https://doi.org/10.1016/S0098-8472(01)00114-9

Raven, P. H., Evert, R. F., & Eichhorn, S. E. (2005). *Biology of plants* (7th ed.). New York: W. H. Freeman and Co.

Reynolds, T. (2004). *Aloes "The genus Aloe"* (p. 408). USA: CRC Press LLC.

Reynolds, T., & Dweck, A. C. (1999). *Aloe vera* leaf gel: A review update. *Journal of Ethnopharmacology*, *68*, 3–37. https://doi.org/10.1016/S0378-8741(99)00085-9

Ripley, B. S., Abraham, T., Klak, C., & Cramer, M. D. (2013). How succulent leaves of Aizoaceae avoid mesophyll conductance limitations of photosynthesis and survive drought. *Journal of Experimental Botany*, *64*, 5485–5496. https://doi.org/10.1093/jxb/ert314

Rodríguez-González, V. M., Femenia, A., González-Laredo, R. F., Rocha-Guzmán, N. E., Gallegos-Infante, J. A., Candelas-Cadillo, M. G., … Rosselló, C. (2011). Effects of pasteurization on bioactive polysaccharide acemannan and cell wall polymers from *Aloe barbadensis* Miller. *Carbohydrate Polymers*, *86*, 1675–1683. https://doi.org/10.1016/j.carbpol.2011.06.084

Saffer, A. M. (2018). Expanding roles for pectins in plant development. *Journal of Integrative Plant Biology*, *60*, 910–923. https://doi.org/10.1111/jipb.12662

Schmidt, J. E., & Kaiser, W. M. (1987). Response of the succulent leaves of *Peperomia magnoliaefolia* to dehydration: Water relations and solute movement in chlorenchyma and hydrenchyma. *Plant Physiology*, *83*, 190–194. https://doi.org/10.1104/pp.83.1.190

Shi, X. D., Nie, S. P., Yin, J. Y., Que, Z. Q., Zhang, L. J., & Huang, X. J. (2017). Polysaccharide from leaf skin of *Aloe barbadensis* Miller: Part I. Extraction, fractionation, physicochemical properties and structural characterization. *Food Hydrocolloids*, *73*, 176–183. https://doi.org/10.1016/j.foodhyd.2017.06.039

Smart, R. E., & Bingham, G. E. (1974). Rapid estimates of relative water content. *Plant Physiology*, *53*, 258–260. https://doi.org/10.1104/pp.53.2.258

Sørensen, I., Pedersen, H. L., & Willats, W. G. T. (2009). An array of possibilities for pectin. *Carbohydrate Research*, *344*, 1872–1878. https://doi.org/10.1016/j.carres.2008.12.008

Stancato, G. C., Buckeridge, M. S., & Mazzafera, P. (2001). Effect of a drought period on the mobilisation of non-structural carbohydrates, photosynthetic efficiency and water status in an epiphytic orchid. *Plant Physiology and Biochemistry*, *39*, 1009–1016. https://doi.org/10.1016/S0981-9428(01)01321-3

Surridge, C. (2019). Uncovering cryptic CAM. *Nature Plants*, *5*, 3. https://doi.org/10.1038/s41477-018-0351-2

Talmadge, J., Chavez, J., Jacobs, L., Munger, C., Chinnah, T., Chow, J. T., … Yates, K. M. (2004). Fractionation of *Aloe vera* L. Inner gel, purification and molecular profiling of activity. *International Immunopharmacology*, *4*, 1757–1773. https://doi.org/10.1016/j.intimp.2004.07.013

Vandenbosch, K. A., Bradley, D. J., Knox, J. P., Perotto, S., Butcher, G. W., & Brewin, N. J. (1989). Common components of the infection thread matrix and the intercellular space identified by immunocytochemical analysis of pea nodules and uninfected roots. *The European Molecular Biology Organization Journal*, *8*, 335–341. https://doi.org/10.1002/j.1460-2075.1989.tb03382.x

Verhertbruggen, Y., Marcus, S. E., Haeger, A., Ordaz-Ortiz, J. J., & Knox, J. P. (2009). An extended set of monoclonal antibodies to pectic homogalacturonan. *Carbohydrate Research*, *344*, 1858–1862. https://doi.org/10.1016/j.carres.2008.11.010

Wiebe, H. H., & Al-Saadi, H. A. (1976). Matric bound water of water tissue from succulents. *Physiologia Plantarum*, *36*, 47–51. https://doi.org/10.1111/j.1399-3054.1976.tb05026.x

Willats, W. G. T., Knox, J. P., & Mikkelsen, J. D. (2006). Pectin: New insights into an old polymer are starting to gel. *Trends in Food Science & Technology*, *17*, 97–104. https://doi.org/10.1016/j.tifs.2005.10.008

Willats, W. G. T., Limberg, G., Buchholt, H. C., Van Alebeek, G. J., Benen, J., Christensen, T. M., … Knox, J. P. (2000). Analysis of pectic epitopes recognised by hybridoma and phage display monoclonal antibodies using defined oligosaccharides, polysaccharides, and enzymatic degradation. *Carbohydrate Research*, *327*, 309–320. https://doi.org/10.1016/S0008-6215(00)00039-2

Willats, W. G. T., Marcus, S. E., & Knox, J. P. (1998). Generation of a monoclonal antibody specific to (1-5)-beta-l-arabinan. *Carbohydrate Research*, *308*, 149–152. https://doi.org/10.1016/S0008-6215(98)00070-6

Willats, W. G. T., Mccartney, L., Mackie, W., & Knox, J. P. (2001). Pectin: Cell biology and prospects for functional analysis. *Plant Molecular Biology*, *47*, 9–27. https://doi.org/10.1023/A:1010662911148

von Willert, D. J., Eller, B. M., Werger, M. J. A., & Brinckmann, E. (1990). Desert succulents and their life strategies. *Vegetatio*, *90*, 133–143. https://doi.org/10.1007/BF00033023

von Willert, D. J., Eller, B. M., Werger, M. J. A., Brinckmann, E., & Ihlenfeldt, H.-D. (1992). *Life strategies of succulents in deserts: With special reference to the Namib Desert*. Cambridge University Press.

Yates, E. A., Valdor, J.-F., Haslam, S. M., Morris, H. R., Dell, A., Mackie, W., & Knox, J. P. (1996). Characterization of carbohydrate structural features recognized by anti-arabinogalactan-protein monoclonal antibodies. *Glycobiology*, *6*, 131–139. https://doi.org/10.1093/glycob/6.2.131

Zhang, X., Rogowski, A., Zhao, L., Hahn, M. G., Avci, U., Knox, J. P., & Gilbert, H. J. (2014). Understanding how the complex molecular architecture of mannan-degrading hydrolases contributes to plant cell wall degradation. *Journal of Biological Chemistry*, *289*, 2002–2012. https://doi.org/10.1074/jbc.M113.527770

SUPPORTING INFORMATION

Additional supporting information may be found online in the Supporting Information section at the end of the article.

Figure S1. CoMPP analysis of hydrenchyma tissue in six *Aloe* species pre- and post- drought stress, with control treatments. Vouchers are deposited in Herbarium C at the Natural History Museum of Denmark. XG = Xyloglycan. Antibodies are listed in Figure 3 in the main part of the study.

Figure S2. COS488 labelling of leaf hydrenchyma in *Aloe helenae* in (a) watered and (b) drought-stressed (b) specimens. Hydrenchyma cell walls are labelled with COS488 but the labelling is significantly reduced in the drought-stressed hydrenchyma, but chlorenchyma is unaffected.

Figure S3. Detection of the RG-I side chains in *Aloe* leaves using LM5 and LM6 monoclonal antibodies (a) Staining with LM5 (green signal) recognizing (1,4)-!-Dgalactan shows a discontinued pattern in chlorenchyma tissue; (b) staining with LM6 (green signal) recognizing (1,5)-"-L-arabinan show instances of sporadic binding in chlorenchyma tissue. Calcofluor White was used as counter stain.

Figure S4. Specificity analysis of anti-mannan antibodies. Calcofluor White (staining (1,4)-β-glucans, blue signal) is used on all sections. Antibodies used are CCRC-M170 binding acetylated mannan (a-c), BS-400-4 binding (1,4)-β-D-mannan (d-f) and LM21 binding (1–4)- β-D-mannan/galactomannan/glucomannan (g-i). Sections were treated with mannanase (b, e, h) and 200 mM NaOH (c, f, i). Mannanase treatment diminishes staining for all antibodies (b, e, h). De-acetylation partially diminishes binding of CCRC-M170 (c), strongly binding of BS-400-4 (f), and minor changes are seen for LM21 (i).

Figure S5. Probing of tissue streaks with CCRC-M170 and LM21 monoclonal antibodies confirms the granular or compartmentalised mannan accumulation in *Aloe* hydrenchyma.

How to cite this article: Ahl LI, Mravec J, Jørgensen B, Rudall PJ, Rønsted N, Grace OM. Dynamics of intracellular mannan and cell wall folding in the drought responses of succulent *Aloe* species. *Plant Cell Environ*. 2019;42:2458–2471. https://doi.org/10.1111/pce.13560